Int J Clin Exp Pathol 2018;11(3):1123-1134
www.ijcep.com /ISSN:1936-2625/IJCEP0070742

Original Article

Potential targets and clinical value of miR-490-5p in hepatocellular carcinoma: a study based on TCGA, qRT-PCR and bioinformatics analyses

Hong Yang[1*], Lu Zhang[2*], Xiao-Dong Wang[1], Meng-Lan Huang[2], Peng Lin[1], Yu-Yan Pang[2], Zhen-Bo Feng[2], Gang Chen[2]

Departments of [1]Medical Ultrasonics, [2]Pathology, The First Affiliated Hospital of Guangxi Medical University, Nanning, People's Republic of China. [*]Equal contributors.

Received December 11, 2017; Accepted January 7, 2018; Epub March 1, 2018; Published March 15, 2018

Abstract: Objective: To explore potential targets and clinical value of miR-490-5p in the oncogenesis and progression of hepatocellular carcinoma (HCC). Methods: Clinical value of miR-490-5p was accessed through The Cancer Genome Atlas (TCGA) and qRT-PCR analyses. Potential target mRNAs of miR-490-5p were predicted by bioinformatics methods and were annotated as Gene Ontology (GO) function analysis, Kyoto Encyclopedia of Genes and Genomes (KEGG) signaling pathway analysis, and Protein-Protein Interaction (PPI) network analysis. Results: miR-490 expression in HCC tissues was lower compared with normal control tissues based on TCGA and down regulation of miR-490-5p was verified by qRT-PCR ($P<0.0001$). Both miR-490 and miR-490-5p had moderate ability to diagnose HCC tissues from noncancerous tissues. Moreover, lower miR-490 level predicted poorer overall survival in patients with HCC ($P=0.0063$). One hundred and eighty-four mRNAs were selected as potential targets of miR-490-5p by overlap with 4,090 prediction genes and 1,478 differentially expressed genes (DEGs). Gene Ontology (GO) function analysis showed that the most significant terms were vasculature development, endoplasmic reticulum, and protein binding in biological process (BP), cellular component (CC), and molecular function (MF). In KEGG signaling pathway analysis, the statistically significant terms were lysosome, focal adhesion, glioma. In PPI network analysis, SRC, SRP9, PDGFRB, RPL28, and RPS23 were identified as the hub genes. Conclusion: miR-490-5p is down-regulated in HCC and may be a prospectively diagnostic and prognostic biomarker. Moreover, miR-490-5p might directly target SRC, SRP9, PDGFRB, RPL28, or RPS23 and play an important role in HCC.

Keywords: Hepatocellular carcinoma, miR-490-5p, bioinformatics analyses

Introduction

Liver cancer is one of the most common malignant tumors in the world. As stated by the latest Global Cancer Statistics, a grand total of 782,500 estimated new liver cancer cases and 745,500 estimated deaths worldwide were reported during the year 2012 [1]. Furthermore, an estimated 40,710 new cases and 28,920 deathsoccurred in liver and intrahepatic bile duct cancers in the United Statesduring the year 2017 [2]. Most (70% to 90%) primary liver cancers are hepatocellular carcinoma (HCC). HCCs descend from hepatocytes and often have poor prognosis. Until now, liver resection is the ideal option for the treatment of HCC [3-8]. However, novel diagnostic and prognostic biomarkers for HCC are also important and necessary [9-13].

MicroRNAs (miRNAs) are one of the types of small non-coding RNAs which can regulate the expression of post-transcriptional gene. According to previous studies, miRNAs take part in various biological processes, such as cell proliferation, migration, invasion, and apoptosis [14-18]. MicroRNA-490 (miR-490) locates on chromosome 7q33. Previous studies have discovered that miR-490-5p was de-regulated in several cancers. For example, Chen et al. found that miR-490-5p expression level in renal cell carcinoma tissue was lower than adjacent normal tissues [19]. Lan et al. and Li et al. both discovered that expression of miR-490-5p was

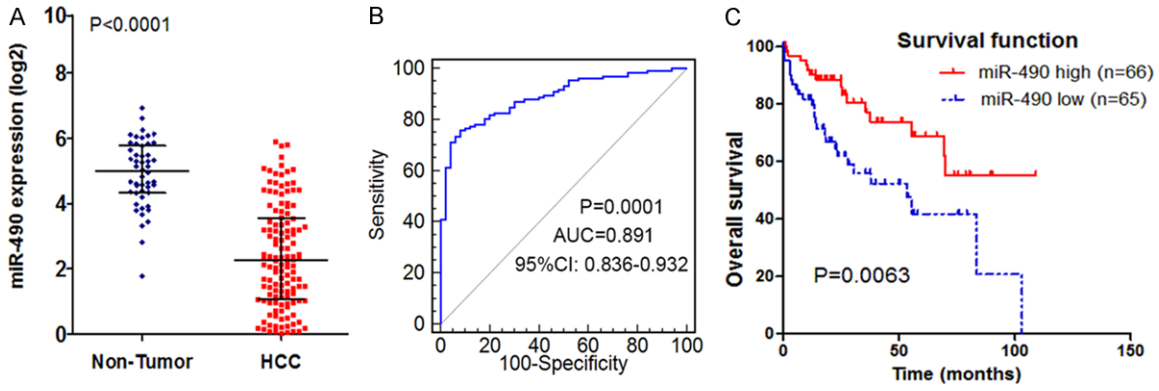

Figure 1. Clinical value of miR-490 in HCC based on TCGA data. A. miR-490 expression in HCC tissues compared with the noncancerous tissues; B. ROC curve analysis of miR-490 for identifying HCC tissues from noncancerous tissues; C. Kaplan-Meier survival curve shows the relationship between miR-490 and the prognosis of patients with HCC.

Table 1. Relationships between miR-490 expression and the clinicopathological parameters in HCC based on TCGA

Clinicopathological feature	n	miR-490-5p expression (Mean±SD)	P
Tissue			
HCC	131	2.39±1.57	
Normal Control	50	4.91±1.02	<0.0001
Gender			
Male	93	2.34±1.48	
Female	38	2.52±1.78	0.559
Age (years)			
<60	73	2.39±1.60	
≥60	58	2.40±1.54	0.983
Grade			
I-II	84	2.57±1.62	
III-IV	46	2.07±1.45	0.083
Stage			
I-II	90	2.38±1.54	
III-IV	29	2.29±1.66	0.795
T Stage			
TX	1	3.17	
T1	67	2.54±1.43	
T2-4	62	2.17±1.67	0.36
N Stage			
NX	40	2.34±1.69	
N0	90	2.42±1.53	0.781
M Stage			
MX	38	2.33±1.59	
M0	91	2.43±1.58	
M1	2	2.01±1.50	0.887
Vascular invasion			

down-regulated in bladder cancer tissues and cells [20, 21]. While in HCC, Chen et al. found that miR-490-5p expression was down-regulated, and it could target ROBO1 to inhibit HCC cell proliferation, migration, and invasion [22]. Lower expression of miR-490-5p was also detected in HCC tissues and cells by Xu et al., and they found that miR-490-5p could target BUB1 and then regulate the TGFβ/Smad signaling pathways [23]. However, the function of miR-490-5p in the oncogenesis and progression of HCC is still not fully elucidated. Moreover, small sample size and individual studies have resulted ininconsistent outcomes about the targets of miR-490-5p.

In the present study, we analyzed the expression level of miR-490-5p through data from The Cancer Genome Atlas (TCGA) and then verified by Reverse Transcription-quantitative real-time PCR (qRT-PCR). Meanwhile, we applied twelve miRNA-target prediction tools to predict the potential miR-490-5p target genes. Gene Ontology (GO) function analysis, Kyoto Encyclopedia of Genes and Genomes (KEGG) signaling pathway analysis, and Protein-Protein Interaction (PPI) networks analysis of potential miR-490-5p target mRNAs were performed to investigate the related signaling pathways of miR-490-5p target genes and miR-490-5p potential molecular mechanisms in HCC.

Materials and methods

Collecting and processing the data from TCGA

We searched and downloaded data of 131 HCC cases and 50 non-cancer cases that involved

Yes	32	2.48±1.74	
No	80	2.42±1.48	0.853
Alcohol consumption			
Yes	35	2.36±1.44	
No	91	2.45±1.60	0.762
Smoking			
Yes	8	2.31±1.50	
No	118	2.43±1.56	0.824
HBV infection			
Yes	48	2.30±1.41	
No	78	2.51±1.63	0.464
HCV infection			
Yes	22	2.35±1.36	
No	104	2.44±1.59	0.793

miR-490-5p expression and included clinicopathological data on TCGA liver HCC. Clinicopathological data such as gender, age, grade, stage, TNM stage, vascular invasion, alcohol consumption, smoking, HBV infection, HCV infection and Overall Survival (OS) [24-26] were obtained. The gene expression data of miR-490-5p was calculated as Log2. Up-regulated Differentially Expressed Genes (DEGs) between HCC tissues and noncancerous tissues were acquired by Gene Expression Profiling Interactive Analysis (GEPIA, http://gepia.cancer-pku.cn/), a visual tool to analyze the data from TCGA [27]. In GEPIA analysis, ANOVA was used as the method, the cut off value of Log2FC was more than one, and the cut off value of q-value was 0.05.

Total RNA extraction and qRT-PCR

Total RNA was extracted from 41 HCC samples and corresponding adjacent non-tumor tissues using the Qiagen RNeasy FFPE Kit following the manufacturer's protocol. Quantification of miR-490-5p was performed by Applied Biosystems PCR7900. The sequences of the miR-490-5p were as follows: F: TTTGGTCTCTTCGGGTCATC, R: CTTAGCTGGACGCCTACCTG. For GAPDH, the primers were: F: GTAAGACCCCTGGACCACCA, R: CAAGGGGTCTACATGGCAACT. Expression values were calculated using the $2^{-\Delta Ct}$ method [28, 29].

Collecting and predicting target mRNAs through bioinformatics methods

We predicted the potential target mRNAs of miR-490-5p by 12 online methods including: miRWalk2.0, MirTarBase, TarBase, Targetminer, polymiRTS, RNA22, microRNA org, Pita, mirRNAMAP, Targetscan, miRDB, and Pictar-vert [30]. Four times or more of the gene appears was regarded as the target gene for miR-490-5p.

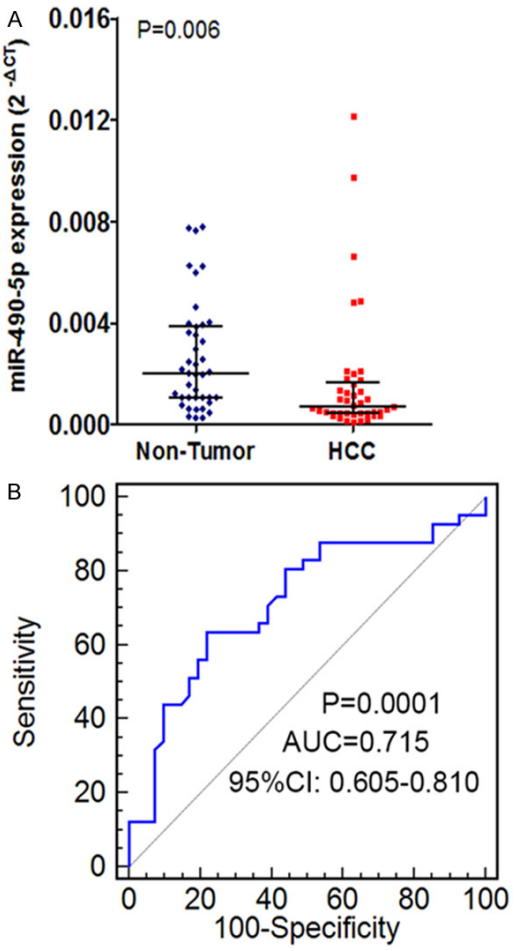

Figure 2. Clinical value of miR-490-5p in HCC based on qRT-PCR data. A. miR-490-5p expression in HCC tissues compared with the corresponding adjacent non-tumor tissues; B. ROC curve analysis of miR-490-5p for identifying HCC tissues from noncancerous tissues.

GO function and KEGG signaling pathway analyses

In order to functionally annotate the potential target mRNAs, we performed a GO function analysis. The GO function terms include Biological Process (BP), Cellular Component (CC), and Molecular Function (MF). Through the KEGG pathway analysis, potential target mRNAs involved in signaling pathways were uncovered.

Table 2. Relationships between miR-490-5p expression and clinicopathological parameters in HCC based on qRT-PCR

Clinicopathological feature		miR-490-5p expression		*P*-value
		High	Low	
		Patients n	Patients n	
Gender	Male	16	14	
	Female	5	6	0.655
Age(years)	≥50	9	14	
	<50	12	6	0.08
Differentiation	High	1	1	
	Moderate	16	14	
	Low	4	5	0.698
TNM stage	I-II	14	7	
	III-IV	7	13	0.043*
Tumor size(cm)	≥5	8	5	
	<5	13	15	0.368
Tumor node	Single	14	11	
	Multiple	7	9	0.444
Cirrhosis	Yes	12	12	
	No	9	8	0.853
Metastasis	Yes	7	13	
	No	14	7	0.043*
Embolus	Yes	3	7	
	No	18	13	0.238
Vascular invasion	Yes	5	7	
	No	16	13	0.431
Capsular invasion	Yes	10	14	
	No	11	6	0.146
AFP	Positive	10	10	
	Negative	8	8	1
NM23	Positive	12	16	
	Negative	9	4	0.116
P53	Positive	11	13	
	Negative	10	7	0.412
P21	Positive	10	7	
	Negative	11	13	0.412
VEGF	Positive	12	15	
	Negative	9	5	0.228
Ki-67	High	8	12	
	Low	13	8	0.161
MVD	High	14	17	
	Low	7	3	0.316

Notes: *P-value<0.05.

A P<0.05 was considered significant. GO function and KEGG signaling pathway analyses were all done with DAVID tools (https://david.ncifcrf.gov/).

PPI network analysis and hub genes identification

In order to construct a PPI network, we uploaded the potential target mRNAs to Search Tool for the Retrieval of Interacting Genes/Proteins (STRING) version 10.5 online tool (http://string-db.org/). Online Tools STRING 10.5 database is widely used to analyze protein interactions. The STRING software is a database containing all known and predicted protein interactions. During PPI network analysis, when a node (represent protein) had lines (representing protein connections) with more than 5 other nodes, it was then identified as a hub gene.

Statistical analysis

The SPSS 22.0 (Armonk, NY, USA analysis, the) and GraphPad Prism 5 (San Diego CA, USA) were used to process the data. P<0.05 was considered significant. TCGA data are shown as the mean ± standard deviation. Student's t-test was used to analyze the differences of miR-490 expression between cancer and non-cancer group and the clinicopathological parameters. qRT-PCR data are shown as median ± quartile range. Wilcoxon signed rank test was used to analyze the differences of miR-490-5p expression between HCC tissues and corresponding adjacent non-tumor tissues, while the clinicopathological parameters analyses were used Chi-square tests. Receiver Operator Characteristic (ROC) curve was established and the Area under the Curve (AUC) with its 95% Confidence Interval (CI) were used to evaluate the diagnostic value of miR-490 and miR-490-5p. The standards for assessing the AUC were: 0.5-0.7 (poor diagnostic ability); 0.7-0.9 (moderate diagnostic ability); 0.9-1.0 (high diagnostic ability). Med-Calc Version 9.2.0.1 (Ostend, Belgium) was used to draw the ROC curves. The prognostic merit of miR-490 in HCC samples was assessed by Kaplan-Meier survival curve. The Kaplan-Meier survival curve was drawn by GraphPad Prism 5.

Table 3. 184 overlapping target mRNAs of miR-490-5p

ZNF581	TAGLN2	SCAMP5	PPT1	NCAPG2	H2AFJ	EMCN	COL15A1	B3GNT5
ZNF28	SUSD4	SAC3D1	PPP1R11	MPC2	GSTA4	EMC4	CLN3	ATP6V1C1
ZIC2	SUB1	RTP4	PPM1G	MKI67	GRK6	EMC2	CKLF	ATP5L
YWHAZ	STC1	RRAGD	PMVK	MARCKS	GPNMB	EIF6	CKAP4	ATP1B1
YBEY	SSR3	RPS23	PLOD1	MAGOHB	GMPS	ECT2	CDKN3	ASPH
WBSCR27	SSR1	RPL28	PLAU	LRP11	GJA5	E2F1	CDH13	ARHGEF39
VBP1	SRP9	ROBO1	PIK3R2	LOXL2	GJA1	DUSP9	CDCA8	ARF3
VAT1	SRC	RNF157	PHLDA3	LASP1	GGH	DTNA	CD34	APOLD1
UBE2A	SPC25	RIPK2	PHF19	LAPTM5	G6PD	DTL	CD24	APOC2
TXNRD1	SOX4	RGS5	PEG10	LAPTM4B	FOXRED2	DTD1	CCDC86	APLN
TSNAX	SMO	RGCC	PECAM1	LAMP2	FOLR2	DLL4	CBR1	AP3B1
TSEN15	SLC35F6	RFWD2	PDIA3	LAMC1	FLVCR1	DCDC2	CAV1	ANO10
TPM3	SLC35B2	RBM8A	PDGFRB	KIAA1522	FKBP9	DAD1	CASK	ANKRD39
TPGS2	SLC29A1	RBBP4	PDGFB	KIAA1462	FBXO32	CYP7A1	CAPRIN1	AGPAT1
TOMM20	SLAMF8	RASSF3	OLA1	IFT52	FBLN1	CYB5R1	CAPN2	ADM2
TMEM50A	SERPINH1	RAB11FIP4	NUSAP1	HSPG2	FANCD2	CXCL9	CANT1	42984
TMEM101	SERPIND1	PYGO2	NRM	HRCT1	FAM83H	CUEDC1	CALM3	
TEAD2	SEMA3G	PXMP4	NREP	HLA-DQA1	FAM127B	CTSC	C8orf33	
TDRKH	SECTM1	PRR11	NOMO2	HLA-DPA1	FABP4	COX8A	C6orf1	
TBC1D16	SCD	PRKDC	NEK2	H3F3A	F5	COL4A2	BUB1	
TAP2	SCARA3	PRC1	NCAPH	H2AFV	ENAH	COL1A2	BCAS4	

Results

miR-490 expression level and clinicopathological parameters in HCC from TCGA

miR-490 expression level in HCC tissues (2.39±1.57) was lower compared with normal control tissues (4.91±1.02), and the difference was statistically significant (P<0.0001) (**Figure 1A**). However, miR-490 expression level and the tested clinicopathological parameters showed no statistically significant relationship (**Table 1**). ROC curve analysis was then performed to evaluate the diagnostic value of miR-490 in HCC. The result showed that miR-490 had moderate ability to diagnose HCC tissues from noncancerous tissues (AUC=0.891, 95%CI: 0.836-0.932, P=0.0001) (**Figure 1B**). Kaplan-Meier survival curve was applied to assess the prognostic merit of miR-490 in HCC samples. The result indicates that lower miR-490 level predicts poorer overall survival in patients with HCC (P=0.0063) (**Figure 1C**).

miR-490-5p expression level and clinicopathological parameters in HCC verified by qRT-PCR

qRT-PCR was applied to verified the expression level of miR-490-5p in HCC, and results exhibited that the expression level of miR-490-5p in HCC was significantly lower than adjacent noncancerous tissues (P=0.006) (**Figure 2A**). The cut-off point was the median value of miR-490-5p expression, and 41 patients were separated into two groups, including high miR-490-5p expression group or low miR-490-5p expression group. Relationships among miR-490-5p expression level and gender, age, differentiation, TNM stage, tumor size, tumor node, cirrhosis, metastasis, embolus, vascular invasion, capsular invasion, alpha fetal protein (AFP) level, NM23 level, p53 level, p21 level, vascular endothelial growth factor (VEGF) level, Ki-67 level, and microvessel density (MVD) were evaluated in 41 HCC samples. The results show that TNM stage and metastasis of HCC are correlated with miR-490-5p expression level (P<0.05). However, miR-490-5p expression level had no relationship with gender, age, differentiation, tumor size, tumor node, cirrhosis, embolus, vascular invasion, capsular invasion, AFP level, NM23 level, p53 level, p21 level, VEGF level, Ki-67 level, and MVD (P>0.05) (**Table 2**). The result of ROC curve analysis also showed that miR-490-5p had moderate diagnostic ability in HCC (AUC=0.715, 95%CI: 0.605-0.810, P=0.0001) (**Figure 2B**).

Table 4. GO function and KEGG signaling pathway analyses of overlapping target mRNAs of miR-490-5p

Sample Group	Rich Factor	*P* value	Gene Number	Description
Biological Process				
GOTERM_BP_ALL	0.04	4.43465E-08	24	Vasculature development
GOTERM_BP_ALL	0.04	7.1525E-08	23	Blood vessel development
GOTERM_BP_ALL	0.04	4.9073E-07	20	Blood vessel morphogenesis
GOTERM_BP_ALL	0.10	1.0705E-06	10	Positive regulation of calcium ion transport
GOTERM_BP_ALL	0.03	2.49522E-06	27	Circulatory system development
GOTERM_BP_ALL	0.03	2.49522E-06	27	Cardiovascular system development
GOTERM_BP_ALL	0.05	3.38281E-06	15	Response to oxygen levels
GOTERM_BP_ALL	0.03	4.95948E-06	26	Positive regulation of transport
GOTERM_BP_ALL	0.05	6.25154E-06	14	Response to hypoxia
GOTERM_BP_ALL	0.05	8.68579E-06	14	Response to decreased oxygen levels
Cellular Component				
GOTERM_CC_ALL	0.03	2.60059E-08	34	Endoplasmic reticulum part
GOTERM_CC_ALL	0.02	1.11833E-07	56	Extracellular vesicle
GOTERM_CC_ALL	0.02	1.13186E-07	56	Extracellular organelle
GOTERM_CC_ALL	0.02	1.6803E-07	67	Vesicle
GOTERM_CC_ALL	0.02	2.1618E-07	65	Membrane-bounded vesicle
GOTERM_CC_ALL	0.02	2.40034E-07	55	Extracellular exosome
GOTERM_CC_ALL	0.02	1.31658E-06	66	Extracellular region part
GOTERM_CC_ALL	0.01	4.02149E-06	109	Cytoplasmic part
GOTERM_CC_ALL	0.01	5.27048E-06	110	Intracellular organelle part
GOTERM_CC_ALL	0.01	6.83878E-06	133	Cytoplasm
Molecular Function				
GOTERM_MF_ALL	0.01	6.15856E-05	132	Protein binding
GOTERM_MF_ALL	0.03	0.003954853	13	Enzyme activator activity
GOTERM_MF_ALL	0.27	0.005104901	3	Platelet-derived growth factor binding
GOTERM_MF_ALL	0.01	0.00823878	155	Binding
GOTERM_MF_ALL	0.06	0.009070104	5	Extracellular matrix structural constituent
GOTERM_MF_ALL	0.02	0.017357428	12	Protein kinase binding
GOTERM_MF_ALL	0.04	0.035405388	5	P-P-bond-hydrolysis-driven transmembrane transporter activity
GOTERM_MF_ALL	0.04	0.035405388	5	Primary active transmembrane transporter activity
GOTERM_MF_ALL	0.03	0.035430144	6	Protein C-terminus binding
GOTERM_MF_ALL	0.02	0.035863615	12	Kinase binding
KEGG Pathway				
KEGG_PATHWAY	0.06	0.004051845	7	Lysosome
KEGG_PATHWAY	0.04	0.00422665	9	Focal adhesion
KEGG_PATHWAY	0.08	0.008855327	5	Glioma

Potential target mRNAs of miR-490-5p

Twelve miRNA-target prediction tools were applied to predict potential miR-490-5p target mRNAs. A total number of 15,623 genes were generated from the prediction process after excluding duplications. In order to increase the credibility of our study, only genes that were predicted by at least four prediction tools were selected for the next analysis and 4,090 were acquired finally. GEPIA was then used as a visual tool to analyze the data in HCC from TCGA. The number of the DEGs in HCC was 1,478 through GEPIA analysis. Then, 184 overlapping genes were selected when they were both in

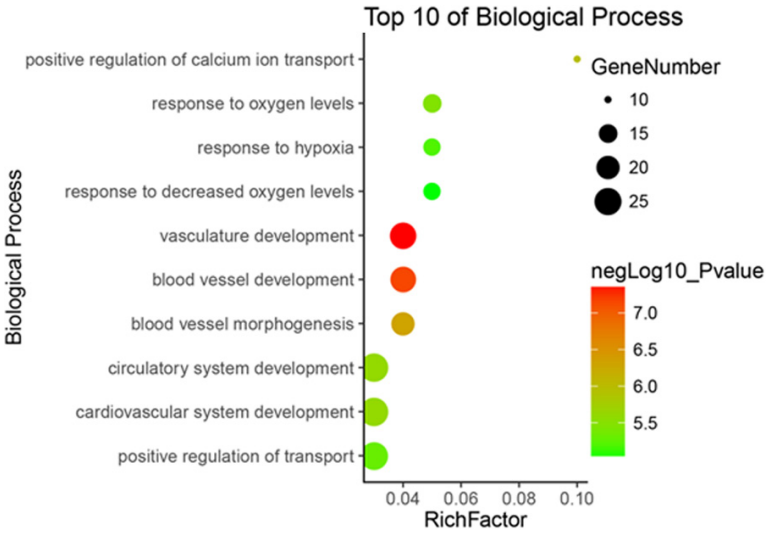

Figure 3. Top 10 Biological Process (BP) analyses of overlapping target mRNAs of miR-490-5p.

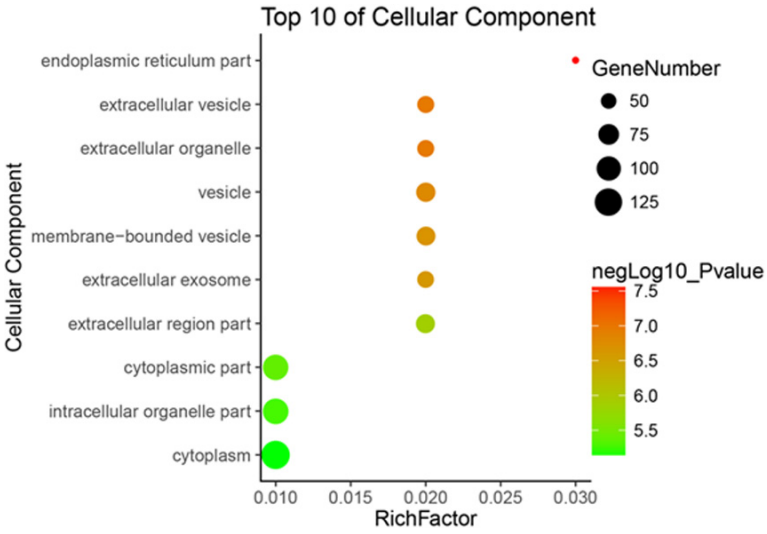

Figure 4. Top 10 Cellular Component (CC) analyses of overlapping target mRNAs of miR-490-5p.

the above 4,090 prediction genes and 1,478 DEGs, as shown in **Table 3**.

GO function and KEGG signaling pathway analyses

GO function analysis classified the 184 overlapping genes into three classifications, containing BP, CC, and MF. In BP analysis, the top three terms which overlapping genes significantly involved in were vasculature development, blood vessel development, and blood vessel morphogenesis. In CC analysis, the top three terms that target genes were significantly enriched in were (endoplasmic reticulum part, extracellular vesicle, and extracellular organelle. In MF analysis, protein binding, enzyme activator activity, and platelet-derived growth factor binding were considered the top three. The top ten terms of GO function analysis are shown in **Table 4** and the visualized GO maps (BP, CC, and MF) are shown in **Figures 3**-**5**. In KEGG signaling pathway analysis, the statistically significant terms were lysosome, focal adhesion, and glioma ($P<0.05$) (**Table 4**).

PPI network analysis and hub genes identification

To explore connections between proteins which encoded by the overlapping genes, a PPI network was built by STRING (**Figure 6**). Five genes which associated with more than five other genes were identified as hub genes in PPI network, including SRC proto-oncogene (SRC), signal recognition particle 9 (SRP9), platelet derived growth factor receptor beta (PDGFRB), ribosomal protein L28 (RPL28), and ribosomal protein S23 (RPS23). The result indicate that SRC, SRP9, PDGFRB, RPL28, and RPS23 have potential to be target genes of miR-490 and might have an important function in the tumor formation and development of HCC.

Discussion

In the present study, the expression level and clinicopathological parameters of miR-490 in HCC were analyzed from TCGA. The result demonstrates that miR-490 is down-regulated in HCC. However, no statistically significant relationship was found between miR-490 expression level and the tested clinicopathological parameters. ROC curve analysis showed that

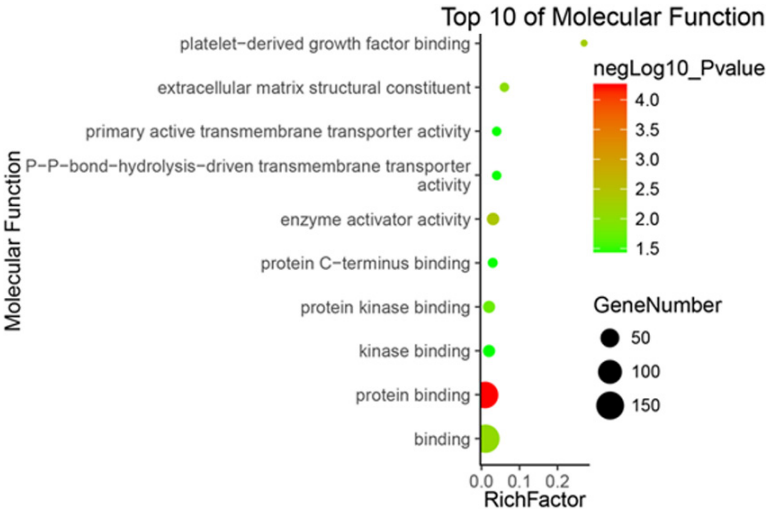

Figure 5. Top 10 Molecular Function (MF) analyses of overlapping target mRNAs of miR-490-5p.

miR-490 had moderate ability to diagnose HCC tissues from noncancerous tissues. Moreover, Kaplan-Meier survival curve analysis indicated that lower miR-490 levels predict poorer overall survival in patients with HCC. We then verified the above results by performing qRT-PCR. In the 41 patients, miR-490-5p was down-regulated in HCC compared with adjacent noncancerous tissues, and it also had a moderate diagnostic ability in HCC. In analysis of clinicopathological parameters, we found that miR-490-5p expression had a correlation with TNM stage and metastasis. Nevertheless, no statistically significant association was found between miR-490 expression level with the gender, age, differentiation, tumor size, tumor node, cirrhosis, embolus, vascular invasion, capsular invasion, AFP level, NM23 level, p53 level, p21 level, VEGF level, Ki-67 level, and MVD.

In the previous study, the investigations of miR-490, including miR-490-3p, and miR-490-5p, were accomplished on various cancers, such as ovarian cancer [31, 32], breast cancer [33, 34], endometrial carcinoma [35], osteosarcoma [36, 37], lung cancer [38, 39], colorectal cancer [40, 41], gastric cancer [42], renal cell carcinoma [19], and bladder cancer [20, 21]. In ovarian cancer, Wang et al. discovered that DLEU1 influenced tumorigenesis and development of ovarian carcinoma by targeting miR-490-3p/CDK1 axis [31], while Tian et al. found that miR-490-3p was down-regulated in cisplatin-resistant ovarian cancer tissues and sensitizes ovarian cancer cells to cisplatin by directly targeting ABCC2 [32]. In lung cancer, Li et al. discovered that miR-490-3p regulated lung cancer metastasis and PCBP1 was a *bona fide* target of miR-490-3p [38], while Gu et al. found that miR-490-3P targeted CCND1 and could inhibit proliferation of lung cancer cells [39]. In colorectal cancer, Zheng et al. investigated miR-490-3p and their results recommended that the miR-490-3p/FRAT1/β-catenin axis is vital in colorectal cancer progression [40], while Xu et al. revealed that miR-490-3p was down-regulated and could inhibit colorectal cancer metastasis by targeting TGFβR1 [41]. In renal cell carcinoma, Chen et al. found that miR-490-5p targeted PIK3CA and functioned as a tumor suppressor [19]. In bladder cancer, Lan et al. found that miR-490-5p could inhibit cell proliferation, invasion, and induce cell apoptosis viaaiming c-FOS [20], while Li et al. discovered that miR-490-5p was down-regulated in human bladder cancer tissues and cell lines and could inhibit cell proliferation also by targeting c-FOS [21]. Reviewing the above published studies, we conclude that miR-490-3p and miR-490-5p play vital roles in various cancers by targeting multiple signaling pathways and mRNAs.

miR-490-3p and miR-490-5p have been also reported in HCC. For example, Zhang et al. revealed that miR-490-3p was up-regulated in HCC tissues and cells [43]. Chen et al. found that miR-490-5p expression was down-regulated in HCC compared with noncancerous tissues [22]. Xu et al. discovered that miR-490-5p expression was down-regulated in HCC tissues and cells [23]. However, the role of miR-490-5p in oncogenesis and progression of HCC is still not fully elucidated and small sample size and individual studies caused inconsistent outcomes regarding the targets of miR-490-5p. Therefore, bioinformatic analyses can play a vital role in predicting the target mRMAs of miR-490-5p.

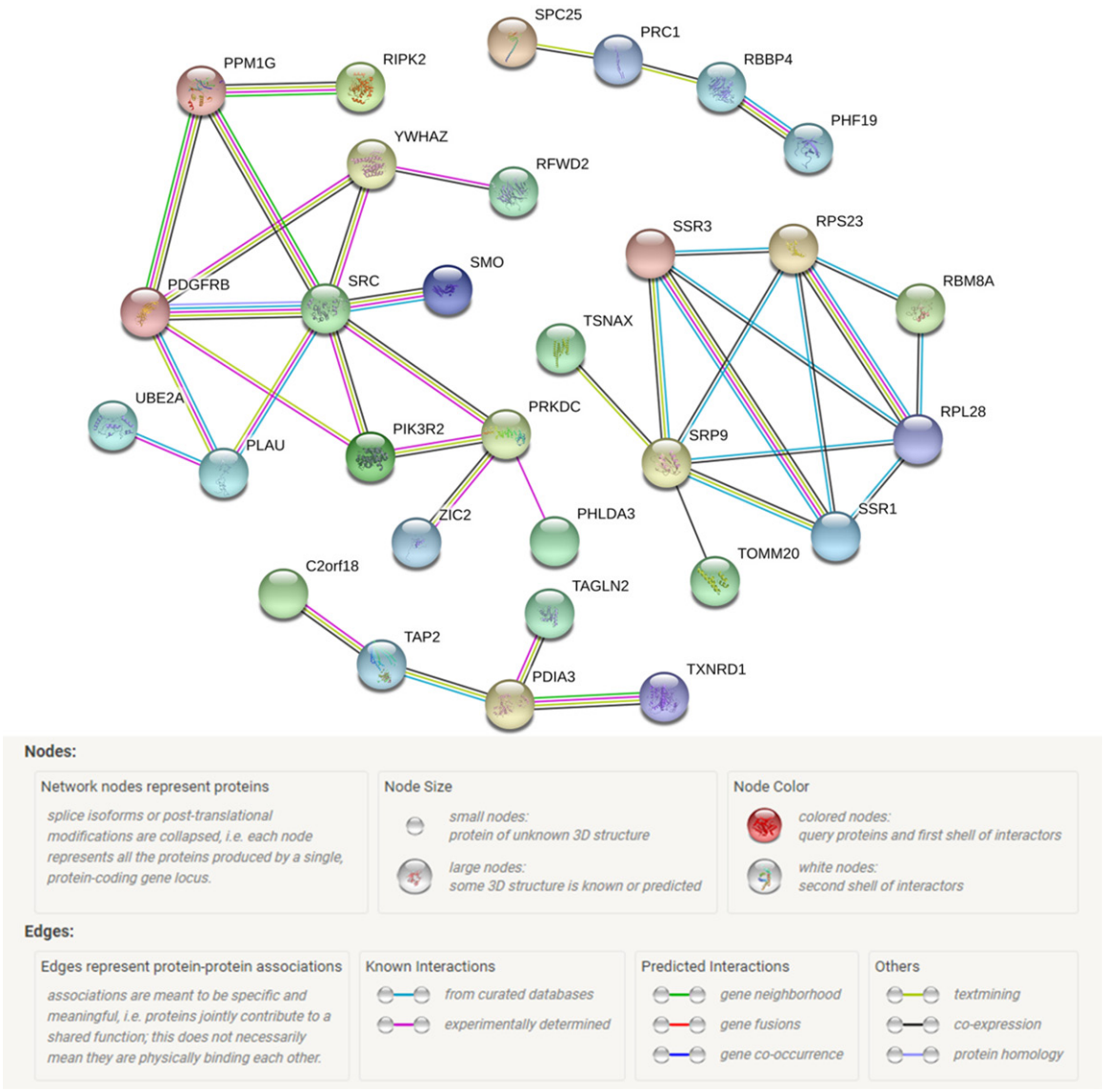

Figure 6. Protein-Protein Interaction (PPI) network of the overlapping target mRNAs of miR-490-5p from STRING online database (http://string-db.org).

We applied twelve miRNA-target prediction tools to predict potential miR-490-5p target mRNAs in this study. Only genes that were predicted by at least four prediction tools were selected for the next analysis. Then, the predicted mRNAs were overlapped with the DEGs in HCC through GEPIA analysis. Finally, 184 overlapping genes were acquired for the next GO function and KEGG signaling pathway analyses and PPI network analysis. Regarding BP analysis, the overlapping target genes were significantly enriched in vasculature development, blood vessel development, and blood vessel morphogenesis, indicating the potential target genes of miR-490-5p may be participate in angiogenesis and influence metastasis of HCC. Regarding CC analysis, endoplasmic reticulum, extracellular vesicle, extracellular organelle, vesicle, membrane-bounded vesicle, and extracellular exosome were terms which the overlapping target genes were significantly involved in. This result demonstrated possible vesicle-associated metabolism. Regarding MF analysis, the overlapping target genes were those associated with protein binding, platelet-derived growth factor binding, protein kinase binding, protein C-terminus binding, and kinase binding, indicated the overlapping target genes

have the high binding ability in molecular function. Moreover, in the KEGG signaling pathway analysis, the overlapping target genes were significantly focused on lysosome, focal adhesion, and glioma. Finally, PPI network analysis of the overlapping target mRNAs was performed, the result showed a complex connection of the proteins encoded by the overlapping target mRNAs by each other. In PPI network analysis, five hub genes were identified, including SRC, SRP9, PDGFRB, RPL28, and RPS23. The result indicates that five hub genes have potential to be targets of miR-490-5p and might play a vital role in the oncogenesis and progression of HCC.

Conclusion

In conclusion, our study explored the expression level and clinicopathological parameters of miR-490 in HCC based on TCGA and then verified miR-490-5p expression level and clinicopathological parameters through qRT-PCR. Both the TCGA result and qRT-PCR result confirmed down-regulation of miR-490-5p in HCC tissues compared with adjacent noncancerous tissues. The qRT-PCR result confirmed the relationships of the miR-490-5p expression level with TNM stage and metastasis. Bioinformatics analyses were applied to predict the potential target mRNAs and signaling pathways of miR-490-5p in HCC. Five hub genes, including SRC, SRP9, PDGFRB, RPL28, and RPS23, were identified potential target genes of miR-490-5p and might play a vital role in the oncogenesis and progression of HCC. Further research may concentrate on the relationship of miR-490-5p with SRC, SRP9, PDGFRB, RPL28, and RPS23, the same as the molecular mechanisms of miR-490-5p in HCC.

Acknowledgements

The study was supported partly by the National Natural Science Foundation of China (NSFC81560386) and Youth Science Foundation of Guangxi Medical University (GXMUYSF201624).

Disclosure of conflict of interest

None.

Address correspondence to: Zhen-Bo Feng and Yu-Yan Pang, Department of Pathology, The First Affiliated Hospital of Guangxi Medical University, 6 Shuangyong Road, Nanning 530021, Guangxi Zhuang Autonomous Region, P. R. China. Fax: +86 771 5352194; E-mail: Fengzhenbo_GXMU@163.com (ZBF); hornor159@126.com (YYP)

References

[1] Torre LA, Bray F, Siegel RL, Ferlay J, Lortet-Tieulent J and Jemal A. Global cancer statistics, 2012. CA Cancer J Clin 2015; 65: 87-108.

[2] Siegel RL, Miller KD and Jemal A. Cancer statistics, 2018. CA Cancer J Clin 2018; 67: 7-30.

[3] Zhang L, Jia G, Shi B, Ge G, Duan H and Yang Y. PRSS8 is downregulated and suppresses tumour growth and metastases in hepatocellular carcinoma. Cell Physiol Biochem 2016; 40: 757-769.

[4] Zhang JY, Weng MZ, Song FB, Xu YG, Liu Q, Wu JY, Qin J, Jin T and Xu JM. Long noncoding RNA AFAP1-AS1 indicates a poor prognosis of hepatocellular carcinoma and promotes cell proliferation and invasion via upregulation of the RhoA/Rac2 signaling. Int J Oncol 2016; 48: 1590-1598.

[5] Jiang H, Zhang X, Tao Y, Shan L, Jiang Q, Yu Y, Cai F and Ma L. Prognostic and clinicopathologic significance of SIRT1 expression in hepatocellular carcinoma. Oncotarget 2017; 8: 52357-52365.

[6] Huang R, Wang X, Zhang W, Zhangyuan G, Jin K, Yu W, Xie Y, Xu X, Wang H and Sun B. Down-regulation of LncRNA DGCR5 correlates with poor prognosis in hepatocellular carcinoma. Cell Physiol Biochem 2016; 40: 707-715.

[7] Yamaguchi M, Osuka S, Weitzmann MN, El-Rayes BF, Shoji M and Murata T. Prolonged survival in hepatocarcinoma patients with increased regucalcin gene expression: HepG2 cell proliferation is suppressed by overexpression of regucalcin in vitro. Int J Oncol 2016; 49: 1686-1694.

[8] Wang F, Yang H, Deng Z, Su Y, Fang Q and Yin Z. HOX antisense lincRNA HOXA-AS2 promotes oncogenesis of hepatocellular carcinoma. Cell Physiol Biochem 2016; 40: 287-296.

[9] Wu Z, Zeng Q, Cao K and Sun Y. Exosomes: small vesicles with big roles in hepatocellular carcinoma. Oncotarget 2016; 7: 60687-60697.

[10] Kassahun WT. Contemporary management of fibrolamellar hepatocellular carcinoma: diagnosis, treatment, outcome, prognostic factors, and recent developments. World J Surg Oncol 2016; 14: 151.

[11] Zheng W, Yao M, Qian Q, Sai W, Qiu L, Yang J, Wu W, Dong Z and Yao D. Oncogenic secretory clusterin in hepatocellular carcinoma: expression at early staging and emerging molecular target. Oncotarget 2017; 8: 52321-52332.
[12] Zhu GQ, Shi KQ, Yu HJ, He SY, Braddock M, Zhou MT, Chen YP and Zheng MH. Optimal adjuvant therapy for resected hepatocellular carcinoma: a systematic review with network meta-analysis. Oncotarget 2015; 6: 18151-18161.
[13] Tu K, Liu Z, Yao B, Han S and Yang W. MicroRNA-519a promotes tumor growth by targeting PTEN/PI3K/AKT signaling in hepatocellular carcinoma. Int J Oncol 2016; 48: 965-974.
[14] Sekhon K, Bucay N, Majid S, Dahiya R and Saini S. MicroRNAs and epithelial-mesenchymal transition in prostate cancer. Oncotarget 2016; 7: 67597-67611.
[15] Wang J, Li Y, Ding M, Zhang H, Xu X and Tang J. Molecular mechanisms and clinical applications of miR-22 in regulating malignant progression in human cancer (Review). Int J Oncol 2017; 50: 345-355.
[16] Wu C, Zhuang Y, Jiang S, Liu S, Zhou J, Wu J, Teng Y, Xia B, Wang R and Zou X. Interaction between Wnt/beta-catenin pathway and microRNAs regulates epithelial-mesenchymal transition in gastric cancer (Review). Int J Oncol 2016; 48: 2236-2246.
[17] Li J, Ju J, Ni B and Wang H. The emerging role of miR-506 in cancer. Oncotarget 2016; 7: 62778-62788.
[18] Gambari R, Brognara E, Spandidos DA and Fabbri E. Targeting oncomiRNAs and mimicking tumor suppressor miRNAs: nuew trends in the development of miRNA therapeutic strategies in oncology (Review). Int J Oncol 2016; 49: 5-32.
[19] Chen K, Zeng J, Tang K, Xiao H, Hu J, Huang C, Yao W, Yu G, Xiao W, Guan W, Guo X, Xu H and Ye Z. miR-490-5p suppresses tumour growth in renal cell carcinoma through targeting PIK3CA. Biol Cell 2016; 108: 41-50.
[20] Lan G, Yang L, Xie X, Peng L and Wang Y. MicroRNA-490-5p is a novel tumor suppressor targeting c-FOS in human bladder cancer. Arch Med Sci 2015; 11: 561-569.
[21] Li S, Xu X, Xu X, Hu Z, Wu J, Zhu Y, Chen H, Mao Y, Lin Y, Luo J, Zheng X and Xie L. MicroRNA-490-5p inhibits proliferation of bladder cancer by targeting c-Fos. Biochem Biophys Res Commun 2013; 441: 976-981.
[22] Chen W, Ye L, Wen D and Chen F. MiR-490-5p Inhibits hepatocellular carcinoma cell proliferation, migration and invasion by directly regulating ROBO1. Pathol Oncol Res 2017; [Epub ahead of print].
[23] Xu B, Xu T, Liu H, Min Q, Wang S and Song Q. MiR-490-5p suppresses cell proliferation and invasion by targeting BUB1 in hepatocellular carcinoma cells. Pharmacology 2017; 100: 269-282.
[24] Liang HW, Yang X, Wen DY, Gao L, Zhang XY, Ye ZH, Luo J, Li ZY, He Y, Pang YY and Chen G. Utility of miR133a3p as a diagnostic indicator for hepatocellular carcinoma: An investigation combined with GEO, TCGA, metaanalysis and bioinformatics. Mol Med Rep 2018; 17: 1469-1484.
[25] Shao P, Sun D, Wang L, Fan R and Gao Z. Deep sequencing and comprehensive expression analysis identifies several molecules potentially related to human poorly differentiated hepatocellular carcinoma. FEBS Open Bio 2017; 7: 1696-1706.
[26] Ding H, Ye ZH, Wen DY, Huang XL, Zeng CM, Mo J, Jiang YQ, Li JJ, Cai XY, Yang H and Chen G. Downregulation of miR1365p in hepatocellular carcinoma and its clinicopathological significance. Mol Med Rep 2017; 16: 5393-5405.
[27] Tang Z, Li C, Kang B, Gao G, Li C and Zhang Z. GEPIA: a web server for cancer and normal gene expression profiling and interactive analyses. Nucleic Acids Res 2017; 45: 98-102.
[28] Liu Y, Ren F, Rong M, Luo Y, Dang Y and Chen G. Association between underexpression of microrna-203 and clinicopathological significance in hepatocellular carcinoma tissues. Cancer Cell Int 2015; 15: 62.
[29] Liu Y, Ren F, Luo Y, Rong M, Chen G and Dang Y. Down-regulation of MiR-193a-3p dictates deterioration of HCC: a clinical real-time qRT-PCR study. Med Sci Monit 2015; 21: 2352-2360.
[30] Dweep H, Gretz N and Sticht C. miRWalk database for miRNA-target interactions. Methods Mol Biol 2014; 1182: 289-305.
[31] Wang LL, Sun KX, Wu DD, Xiu YL, Chen X, Chen S, Zong ZH, Sang XB, Liu Y and Zhao Y. DLEU1 contributes to ovarian carcinoma tumourigenesis and development by interacting with miR-490-3p and altering CDK1 expression. J Cell Mol Med 2017; 21: 3055-3065.
[32] Tian J, Xu YY, Li L and Hao Q. MiR-490-3p sensitizes ovarian cancer cells to cisplatin by directly targeting ABCC2. Am J Transl Res 2017; 9: 1127-1138.
[33] Zhao L and Zheng XY. MicroRNA-490 inhibits oncogenesis and progression in breast cancer. Onco Targets Ther 2016; 9: 4505-4516.
[34] Jia Z, Liu Y, Gao Q, Han Y, Zhang G, Xu S, Cheng K and Zou W. miR-490-3p inhibits the growth and invasiveness in triple-negative breast can-

cer by repressing the expression of TNKS2. Gene 2016; 593: 41-47.
[35] Sun KX, Chen Y, Chen S, Liu BL, Feng MX, Zong ZH and Zhao Y. The correlation between microRNA490-3p and TGFalpha in endometrial carcinoma oncogenesis and progression. Oncotarget 2016; 7: 9236-9249.
[36] Tang B, Liu C, Zhang QM and Ni M. Decreased expression of miR-490-3p in osteosarcoma and its clinical significance. Eur Rev Med Pharmacol Sci 2017; 21: 246-251.
[37] Liu W, Xu G, Liu H and Li T. MicroRNA-490-3p regulates cell proliferation and apoptosis by targeting HMGA2 in osteosarcoma. FEBS Lett 2015; 589: 3148-3153.
[38] Li J, Feng Q, Wei X and Yu Y. MicroRNA-490 regulates lung cancer metastasis by targeting poly r(C)-binding protein 1. Tumour Biol 2016; 37: 15221-15228.
[39] Gu H, Yang T, Fu S, Chen X, Guo L and Ni Y. MicroRNA-490-3p inhibits proliferation of A549 lung cancer cells by targeting CCND1. Biochem Biophys Res Commun 2014; 444: 104-108.
[40] Zheng K, Zhou X, Yu J, Li Q, Wang H, Li M, Shao Z, Zhang F, Luo Y, Shen Z, Chen F, Shi F, Cui C, Zhao D, Lin Z, Zheng W, Zou Z, Huang Z and Zhao L. Epigenetic silencing of miR-490-3p promotes development of an aggressive colorectal cancer phenotype through activation of the Wnt/beta-catenin signaling pathway. Cancer Lett 2016; 376: 178-187.
[41] Xu X, Chen R, Li Z, Huang N, Wu X, Li S, Li Y and Wu S. MicroRNA-490-3p inhibits colorectal cancer metastasis by targeting TGFbetaR1. BMC Cancer 2015; 15: 1023.
[42] Zhou B, Wang Y, Jiang J, Jiang H, Song J, Han T, Shi J and Qiao H. The long noncoding RNA colon cancer-associated transcript-1/miR-490 axis regulates gastric cancer cell migration by targeting hnRNPA1. IUBMB Life 2016; 68: 201-210.
[43] Zhang LY, Liu M, Li X and Tang H. miR-490-3p modulates cell growth and epithelial to mesenchymal transition of hepatocellular carcinoma cells by targeting endoplasmic reticulum-Golgi intermediate compartment protein 3 (ERGIC3). J Biol Chem 2013; 288: 4035-4047.